Reproduced by

DOCUMENT SERVICE CENTER

ARMED SERVICES TECHNICAL INFORMATION AGENCY

U. B. BUILDING, DAYTON, 2, OHIO

REEL-C 7366

A.T.I 208346

"NOTICE: When Government or other drawings, specifications or other data are used for any purpose other than in connection with a definitely related Government procurement operation, the U.S. Government thereby incurs no responsibility, nor any obligation whatsoever; and the fact that the Government may have formulated, furnished, or in any way supplied the said drawings, specifications or other data is not to be regarded by implication or otherwise as in any manner licensing the holder or any other person or corporation, or conveying any rights or permission to manufacture, use or sell any patented invention that may in any way be related thereto."

UNCLASSIFIED

STI ATI No. 208346
ASTIA FILE COPY

U-7537

LIBRARY OF CONGRESS
SCIENCE & TECHNOLOGY PROJECT
TECHNICAL INFORMATION SECTION

Technology Project
Library of Congress
TO BE RETURNED

NOV 26 1948

B

RETURN TO:
ASTIA REFERENCE CENTER
LIBRARY OF CONGRESS
WASHINGTON 25, D.C.

PRINCETON UNIVERSITY

24NOV1948

PRINCETON UNIVERSITY
DEPARTMENT OF PHYSICS

NR061-020

N6ori-105 Task II

TECHNICAL REPORT

Velocity Loss Measurements on Shocks in a Shock Tube

by

R. J. Emrich

LIBRARY OF CONGRESS
SCIENCE & TECHNOLOGY PROJECT
TECHNICAL INFORMATION SECTION

NOV 26 1948

B

Submitted by
Walker Bleakney

Copy No. 4
November 18, 1948

VELOCITY LOSS MEASUREMENTS ON SHOCKS IN A SHOCK TUBE

by

R. J. Emrich
Princeton University and Lehigh University

In the shock tube developed at Princeton(1) as an instrument for the study of transient fluid dynamics, the determination of incident plane shock conditions is accomplished through a knowledge of the temperature and pressure of the undisturbed air and the incident velocity of the shock. The incident velocity is measured by timing the transit of the shock between two stations in the tube preceding the point under study. While a simple theory of flow in the tube indicates that the shock proceeds through the tube with a constant velocity for a time, it is to be expected that dissipative effects operate to cause a gradual decrease in the shock strength and velocity. The presently reported work was undertaken to measure the amount by which the shock velocity decreases in its travel through the tube.

A. APPARATUS AND METHOD

1. Shock tube. A shock tube 15 cm in diameter and 10 meters long was used in this study(2). The 10 meter tube, which is sketched in Fig. 1, consisted of a 1 meter long compression chamber and a 9 meter expansion chamber. These two chambers were locked together, by a removable clamp, with a cellophane diaphragm held between them. Air was pumped

---

1. Walker Bleakney, "Shock Waves in a Tube", Phys. Rev. 69, 678 (1946)
2. The shock tube was designed and erected by W. T. Read and G. T. Reynolds

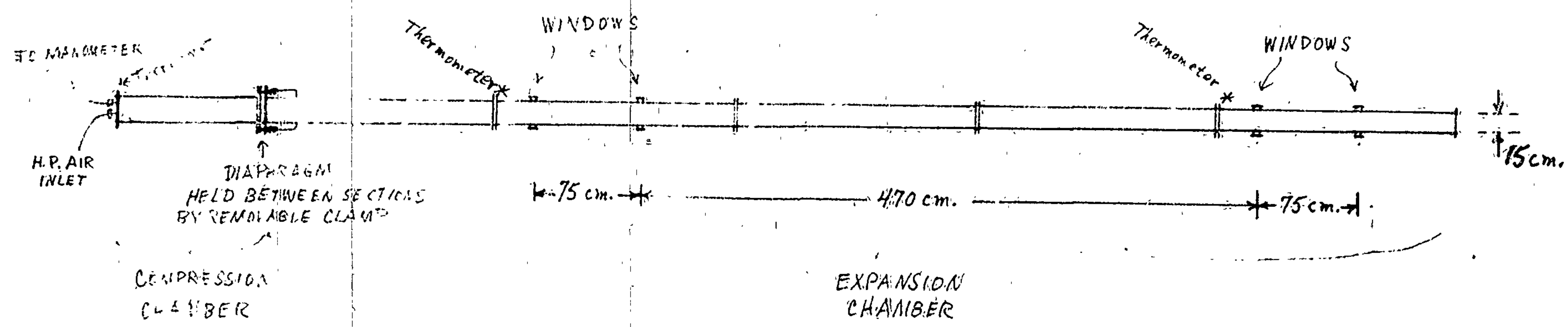

FIG. 1. SHOCK TUBE

into the compression chamber at pressures up to several atmospheres, and the cellophane diaphragm ruptured with an internal knife. In this, as in other shock tubes, the bursting diaphragm releases the high pressure gas from the compression chamber into the expansion chamber, the resulting flow in the expansion chamber consisting of a shock which moves into the undisturbed gas and a mass motion of the air behind the shock away from the compression chamber.

The expansion chamber of the tube was constructed of 1/4" wall brass tubing made in 6 ft. sections bolted together by flanges with rubber sealing gaskets. Two of the sections were fitted with two pairs of window ports each, arranged in such a way that a horizontally directed light beam passed diametrically through the tube at each of the four pairs of windows. These light beams were used to detect the arrival of the shock at the four successive positions as described in the following section.

Each window port consisted of a window support holder soldered to the cut-away tube wall, a window support one inch in diameter with a 3/16" x 3/8" milled slot which fitted into and was fastened to the support holder, and a thin circle of plate glass cemented over the slot in the window support. The inside surface of the shock tube was thus distorted only by a flat 1" diameter recess tangent to the tube surface.

The compression chamber was similarly constructed of a shorter section of brass tubing and provided with a valve to admit high pressure air and a manometer connection.

Mercury-in-glass thermometers were affixed to the tube at three positions; the thermometer bulbs were immersed in mercury contained in steel blocks bolted to the tube flanges. These made it possible to check on the uniformity of temperature of the gas in the tube. The extreme end of the expansion chamber was open to the atmosphere whose pressure and relative humidity were frequently recorded. After each shot, air was blown through the tube to remove the fragments of the burst cellophane diaphragm; this also assured that the humidity of the air in the expansion chamber was that recorded outside.

2. Optical-electronic detection of shock. The optical arrangement for detecting the passage of the shock at any one of the four positions in the tube is shown in Fig. 2, approximately to scale. Light from the incandescent filament is prevented from reaching the phototube, when there is no optical disturbance in the shock tube, by three parallel knife edges adjusted to all meet a single hypothetical plane perpendicular to the tube axis, i. e., parallel to the shock front.

As indicated in the diagrammatic sketch of Fig. 3, which is not to scale, the two knife edges nearest the light source limit the light entering the shock tube to rays slanting slightly toward the direction of shock travel. Until the arrival of the shock, these rays strike the third knife edge and do not reach the phototube. But when the shock enters this region, the rays are totally reflected by the shock which may be thought of as a surface of discontinuity in optical density. The reflected rays are directed slanting back from the direction of shock travel, and, missing the third knife edge, fall on the phototube.

It is assumed in the foregoing description that the light is

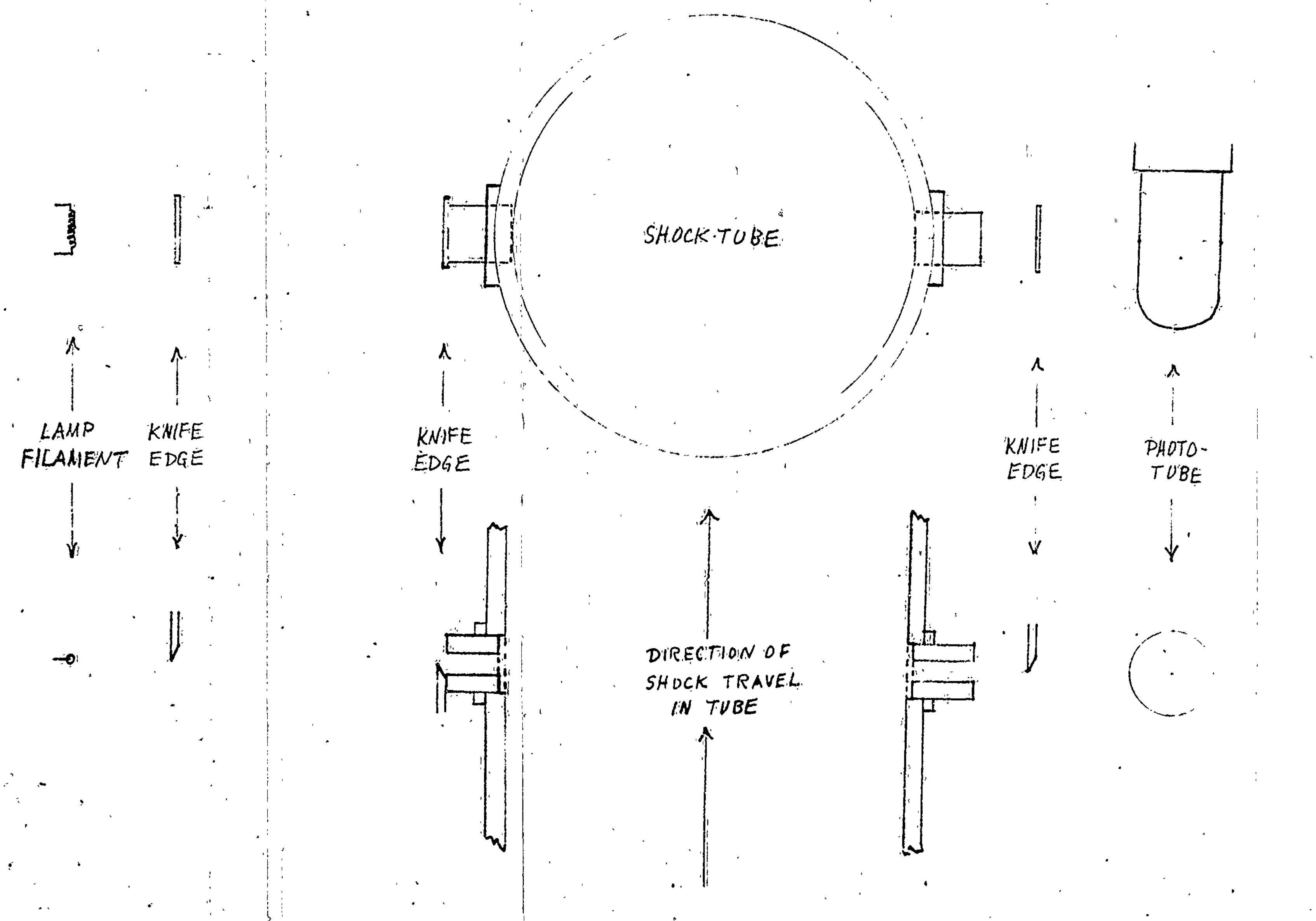

FIG 2. SIDE VIEW AND TOP VIEW OF OPTICAL ARRANGEMENT FOR SHOCK DETECTION.

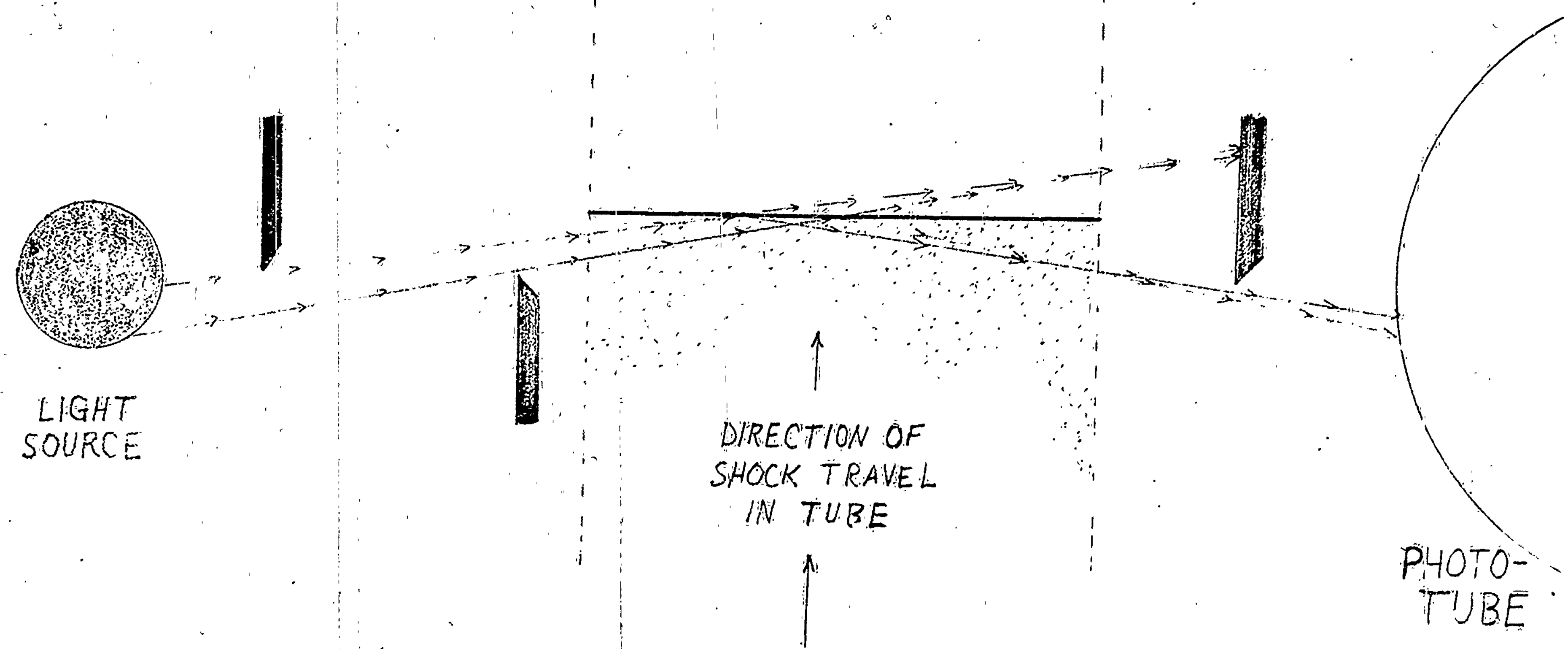

FIG 3. RAY DIAGRAM

propagated in accordance with geometrical optics, and that the shock represents a plane surface of optical discontinuity between two homogeneous media of constant index of refraction. There is no doubt that, under the extremely small angles of deviation which are of interest in the arrangement used (about 1/10 degree), geometrical optics is a poor approximation. Diffraction effects are of appreciable magnitude as can both be demonstrated theoretically[3] and be observed visually. As to whether the shock front is a true plane surface of optical discontinuity to the extent assumed, there is no evidence, except that we have observed the increase of light on the phototube to be usually in accordance with the predictions of this assumption.

The calculation of the rate at which light is reflected to the phototube as the shock moves past the knife edges is readily made when ray optics are used. The result is that, until other edges than the knife edges limit the rays, <u>the light flux reflected to the phototube is proportional to the distance the shock travels beyond the knife edges</u>. We have made no attempt to calculate the relationship between reflected light flux and shock travel by diffraction theory, nor have we calculated the effects of errors in adjusting the knife edges to strict parallelism.

---

3. With a line source at the first knife edge, diffraction theory shows that the first maximum of intensity of the diffraction pattern of the second knife edge at the third knife edge is about 0.02 inch from the geometrical shadow. This corresponds to the distance the shock moves in about one microsecond, and the reflection of all rays meeting the shock front at a grazing angle of less than about 1/10 degree.

In these experiments, the phototube used to detect the changes in light admitted past the knife edges on passage of the shock was a type 931A. A conventional amplifier using high transconductance tubes with low load resistances to preserve the shape of the phototube signal transmitted the signal by cable to a central station. There the signals from all four of the detection stations were applied to the deflecting plates of a cathode-ray oscilloscope tube by means of a mixing stage.

3. Distance and time interval measurement. The distances between detection stations along the tube (see Fig. 1) were determined with an accuracy of better than 0.01 percent by cathetometer settings on the knife edges. The distances remained unchanged during the course of these experiments, except that half of the measurements were made with the detection stations in the positions shown in Fig. 1 and half were made with both shock tube sections fitted with windows at the extreme end of the tube; the distances between knife edges were measured for each of these arrangements independently.

Time intervals between transits were measured with a moving film camera photographing a cathode-ray oscilloscope. A somewhat unusual combination of oscilloscope spot deflection relative to the motion of the film in the camera permitted a 20-fold increase in accuracy of time interval measurement for a given film velocity. This is accomplished, at the risk of obtaining about 5% of the measurements with only a 10-fold increase in accuracy, by sweeping the oscilloscope spot back and forth in a line perpendicular to the direction of film motion and imposing the transit-marking pulses to deflect the oscilloscope spot in the same direction as the film motion.

An example of a record obtained with the apparatus is shown in Fig. 4. In this figure, the horizontal deflection of the spot is a continuous motion from left to right for precisely 50 μ sec followed by motion from right to left for 50 μ sec; the vertical deflection of the spot consists of timing pips 5 μ sec apart with the transit-marking pulses superposed. The resulting record is spread out vertically due to the film motion in the camera. It may be noticed that timing pips occur at the extreme ends of the horizontal sweep. The transit-marking pulses are easily discernible; the time separation between them is measured by counting the number of complete horizontal sweeps between them, corresponding to 100 μ sec each, and measuring the fraction of a sweep at each end of the interval in terms of the 5 μ sec pips. On the original 35 mm film record the intersection of the linear beginning of the transit-marking pulse with the sweep base line can be estimated under a magnifying glass to within 1 μ sec, and with a traveling microscope can be measured to within 0.1 μ sec. When a transit-marking pulse occurs within a few microseconds of the ends of the horizontal sweep, its measurement is not possible to as high an accuracy due to the slightly rounded corners of the horizontal sweep waveform.

The time-control of the sweep and the timing pips were obtained from a 100 KC crystal controlled secondary frequency standard. A 10 KC sinusoidal signal derived from the 100 KC standard frequency was used to synchronize a 10 KC multivibrator at a slightly variable phase; this multivibrator was also provided with a control to vary slightly the relative

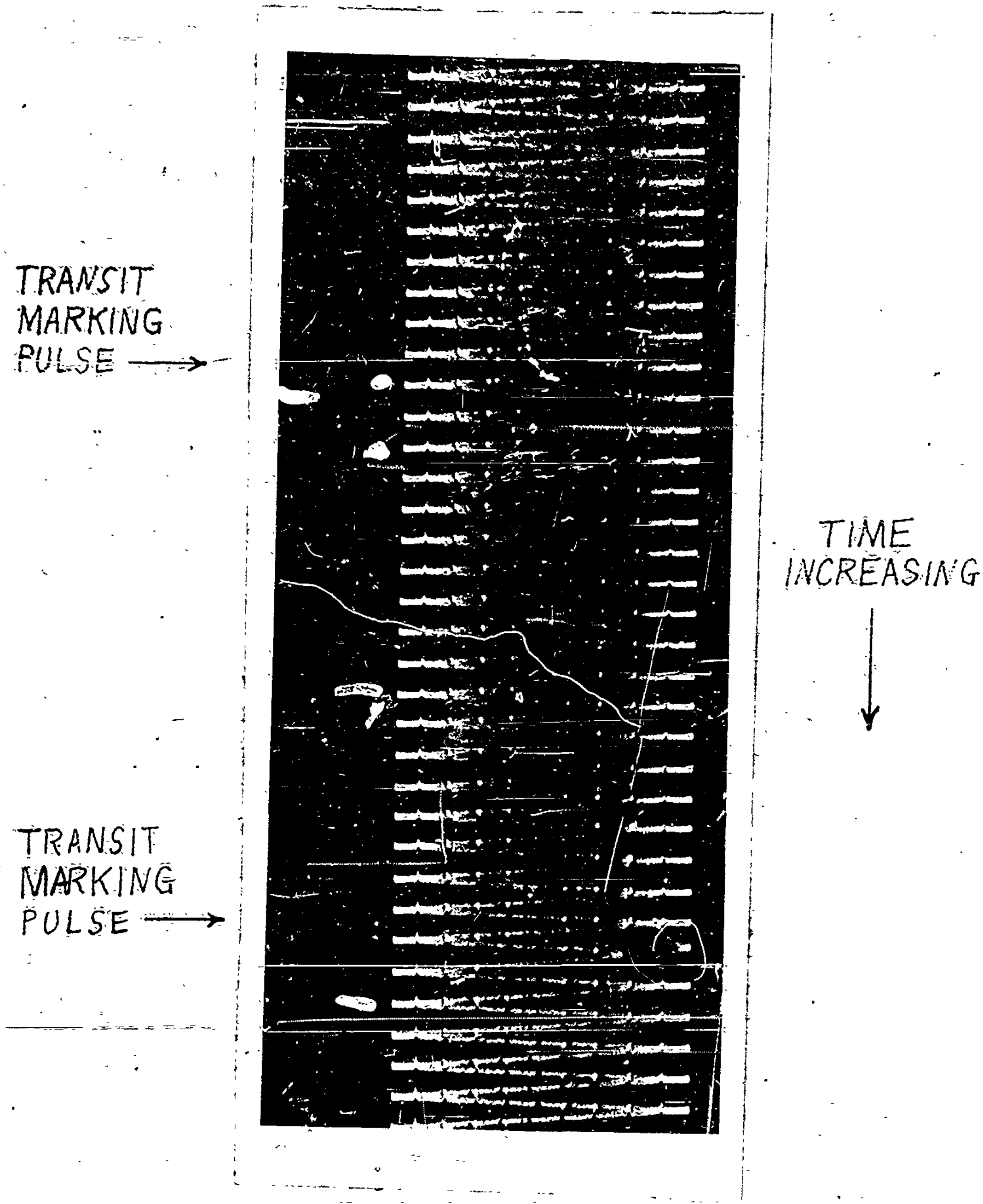

FIG 4. OSCILLOGRAPH TIME RECORD

duration of the two halves of its cycle. The resulting wave form was clipped to produce a square wave which in turn was introduced to a relatively low time-constant filter to produce the waveform desired for the horizontal sweep. The two adjustments mentioned above provided the means to synchronize the sweep with the timing pulses in such a way as to bring timing pulses at the exact ends of the sweep.

A Dumont type 5CP cathode-ray tube with a special low persistence zinc oxide screen was used with 5000 volts on the intensifier. This was photographed with an f/1.9 lens in a General Radio moving film camera modified by replacing the film spools with pulleys to permit a cemented-together endless belt of film 87 cm in length to run in the camera. The intensity grid of the cathode ray tube was maintained at a high negative bias except for a 90 millisecond interval when the bias was reduced nearly to zero for a single exposure of the endless strip of film in the camera. The 90 millisecond rectangular pulse applied to the cathode-ray tube intensity grid was initiated by the passage of the shock over a contactor placed near the diaphragm in the expansion chamber of the shock tube.

B. MEASUREMENTS OF DECREASE OF SHOCK VELOCITY

Various shock strengths are produced in the shock tube by varying the pressure in the compression chamber before rupturing the diaphragm. In the present experiments, shock strengths from as small as could be detected by the optical-electronic pickups to over 10 times the smallest were studied by adjusting the pre-rupture compression chamber pressure to six certain values and timing the transits of the resulting shocks over the four stations arranged as in Fig. 1. The velocity of most of the shocks was found to decrease with travel through the tube, but some of the weakest shocks were found to be moving faster at the further end of the tube than at the end nearest the diaphragm. This anamolous result was presumed to be associated with the mode of formation of the shock upon diaphragm rupture, and all the velocity measurements were repeated with the four detection stations located at the further end of the tube. These measurements showed that shocks of all strengths studied decreased in velocity with travel.

The distance and time measurements are recorded in Table I of the appendix, along with temperature and humidity measurements. From these measurements, the fractional loss in velocity per meter of travel was calculated and the values are represented graphically for various pre-rupture compression chamber pressures(3) in Fig. 5. The vertical intervals plotted about each of the average values include all the measurements made at each initial pressure.

With each of the six pre-rupture compression chamber pressures, and with the detection stations in each of the two arrangements, five or more measurements of shock transit times were made. With the same initial conditions, which resulted in the same shock velocity to within one per cent, the decrease in velocity over the interval varies from shot to shot by just about the same amount as the average decrease itself. While the decrease in velocity over the interval was quite small - of the order of one percent

3. Pressures plotted in Fig. 5 are gauge pressures, i. e., pressure excess over atmospheric.

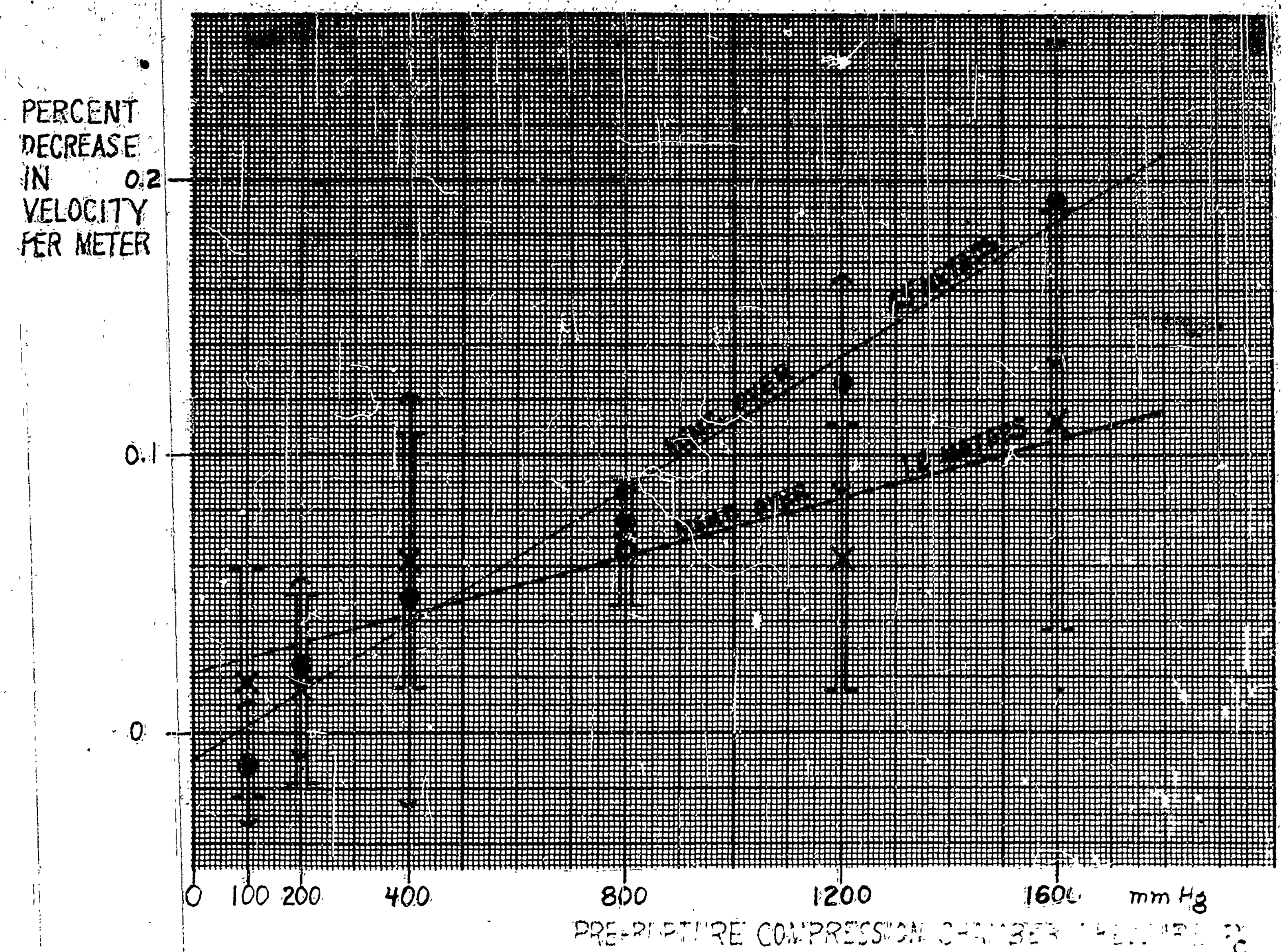

FIG 5. VEL[illegible] LOSS OF VARIOUS STRENGTH [illegible]

of the velocity - it was, except for the weakest shocks, more than ten times the estimated maximum error of measurement; it is believed that there was possibly a real variation in the amount by which a shock of a given strength decreased in velocity.

C. INTERPRETATION OF VELOCITY LOSS DATA IN TERMS OF DECREASE IN SHOCK STRENGTH

A normal shock traveling into undisturbed gas can be described in terms of the pressures and densities on each side of the shock, the gas velocity behind the shock, and the propagation velocity of the shock. These quantities satisfy the Rankine-Hugoniot relations, which, for an ideal gas, yield the relation[4]

$$\frac{V^2}{a^2} = 1 + \frac{\gamma + 1}{2\gamma} z \qquad (1)$$

where V is propagation velocity of shock

γ is ratio of specific heats of gas

$a = \sqrt{\gamma p_1/\rho_1}$ is sound velocity in undisturbed gas

$z = \dfrac{p_2 - p_1}{p_1}$ is shock strength, i. e., the fractional increase in pressure of the gas behind the shock over its value in the undisturbed gas.

Thus, the shock strength z is calculable if V, a, and γ are known, and the measurements of the decrease in V with travel which have been made may be represented in terms of decrease in shock strength with travel.

---

4. See, e. g., Liepmann and Puckett, "Introduction to Aerodynamics of a Compressible Fluid", page 40, Wiley 1947

1. Measurement of Sound Velocity. While the velocity of sound in air has been measured by many observers using quite different methods, the values published differ by more than the experimental errors[5]. In addition, the corrections to be applied for variations in the composition of the air are somewhat indefinite. It was relatively simple, with the apparatus for measuring shock velocities already at hand, to measure sound velocity in the air in the shock tube directly. From this measurement, small variations in temperature and humidity could be allowed for in computing sound velocity.

The measurement of sound velocity was made by placing a steel plate in place of the cellophane diaphragm at the one end of the expansion chamber to act as a reflector, and a microphone composed of a 2 inch diameter tourmaline crystal at the other end. Inside the tube, about 1.5 meters from the microphone, a feeble spark generated a sound pulse which was detected by the microphone first after reaching it directly and second after reflection from the closed end of the tube 8.419 meters distant from the spark. The time interval between the arrival of the direct and reflected pulses was determined by applying the microphone signals to the oscilloscope photographed by the moving film camera.

In air at 25.5°C and or 55% relative humidity, the measured value of sound velocity was 347.4 m/sec[6].

---

5. Alexander Wood, "Acoustics", p. 262, Blackie, 1940.

6. This measurement when adjusted for temperature and humidity by the Regnault formula quoted by Wood, p. 250, gives 330.4 m/sec for sound velocity in dry air at 0°C.

2. Decrease in shock strength with travel. Since the measurements showed that shocks of a given strength decreased in velocity by variable amounts even when the conditions of the tube and gas within the tube were the same, it is only feasible to derive the average decrease in shock strength with travel.

Using 1.40 as the value of γ, the expression (1) gives for the shock strength, z,

$$z = \frac{7}{6}\left(\frac{V^2}{a^2} - 1\right). \qquad (2)$$

Differentiating equation (2) with respect to the position coordinate x, we have for average conditions pertaining during the measurements

$$\frac{dz}{dx} = \frac{7}{3}\frac{V}{a^2}\frac{dV}{dx} = \frac{7}{3}\frac{V^2}{a^2}\cdot\frac{1}{V}\frac{dV}{dx} = \frac{7}{3}\frac{V^2}{a^2}k,$$

and the average fractional decrease in shock strength per meter of travel

$$\frac{1}{z}\frac{dz}{dx} = \frac{2V^2 k}{V^2 - a^2}. \qquad (3)$$

k, the quantity plotted in Fig. 5, is the fractional decrease in velocity V of the shock per meter.

In Table II of the appendix, the average values of the shock velocity, sound velocity, and percent loss of shock velocity per meter are tabulated, the averages computed over the measurements taken with a given pre-rupture compression chamber pressure and arrangement of detection stations; the average sound velocity at each set of conditions has been obtained by adjusting the measured value at 25.5°C and 55% humidity by the Regnault formula[7] for average conditions of temperature and humidity prevailing during the measurements. From these average values, the average shock strength has been computed by means of equation (2) and the fractional decrease in shock strength per meter has been computed from equation (3). In Fig. 6, the latter of these two derived quantities is presented graphically as a function of the former; the vertical intervals on this graph represent the variation in the measured decrease in shock velocity.

D. DISCUSSION OF RESULTS

From Fig. 6 it is seen that shocks decreased in strength by less than 2 percent per meter of travel, and that, on the average, shocks of all strengths studied beyond 7 meters from the diaphragm decreased at the rate of around 0.5 percent per meter of travel.

Comparing the measurements over the longer distance interval with those over the shorter, it appears that the weakest shocks increased in strength at first and then decreased with travel over the longer interval, whereas the strongest shocks decreased in strength more rapidly at the beginning than at the end of the longer interval. Shocks of one intermediate strength ($z = 0.4$) seemed to lose strength at a uniform rate, and these, furthermore, showed less variation in the measured velocity loss over both the 5.5 and 1.8 meter intervals than did shocks of either greater or less strength. An interpretation of these observations may be connected with

7. See footnote 6.

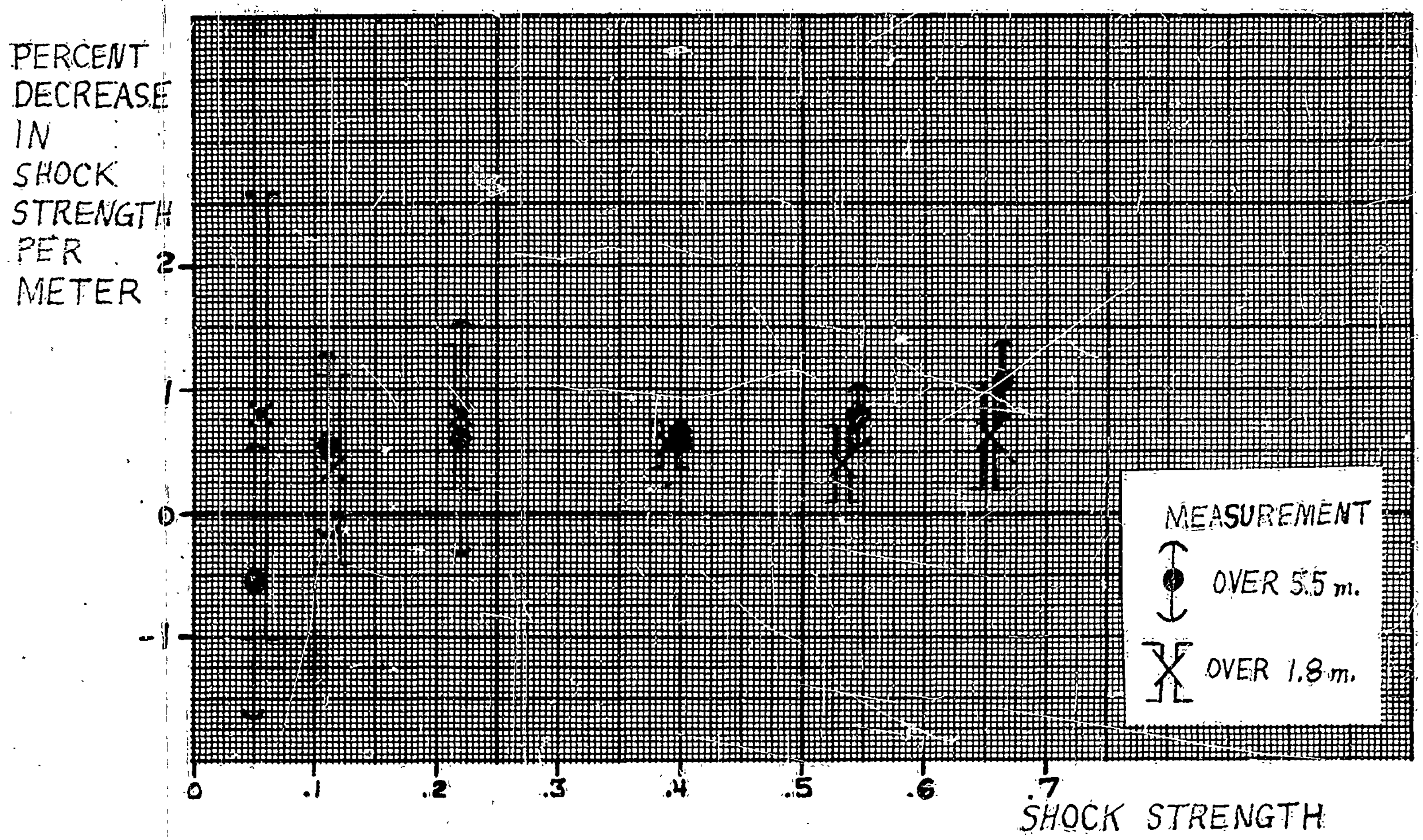

FIG 6. DECREASE IN SHOCK STRENGTH OF VARIOUS STRENGTH SHOCKS

the mode of formation of the shock after diaphragm rupture. A further discussion of the results follows.

1. Attempts to find source of variations in shock strength. Since there were, during the time occupied in performing these measurements, variations in temperature, humidity, and pressure of the air into which the shock moved, a correlation between the velocity loss and these variables has been sought. No such correlation has been found, and in fact, several examples of large differences in velocity loss with no variation in the condition of the undisturbed air may be selected.

An increase in shock velocity over the interval, such as observed with the weakest shocks, can be pictured as a set of one or more shocks, less intense than the main shock and following behind, eventually coalescing with and strengthening the main shock. Such weak secondary shocks might be detected by the optical-electronic stations; however, none was ever recorded. It is not to be expected that secondary shocks would be recorded in the case of the weakest main shock, because the strength of these main shocks was at just about the limit of the detectors. In the case of the stronger main shocks where secondary shocks would be capable of detection, the failure to record any may indicate that any such had already coalesced with the main shock before reaching the first detection station[8].

8. The strongest shocks appear to have decreased in strength more rapidly near the beginning of the 5.5 meter interval than near the end. This could be accounted for by rarefaction waves following behind and coalescing with the main shock; rarefaction waves would not be detected by the optical-electronic pickups.

The sources of secondary shock mentioned in the preceding paragraph might be either of the following:

(1) Reflections from the sides of the shock tube of the initial curved wave front of the disturbance. The cellophane diaphragm bulged under the pre-rupture compression chamber pressure, so that even if it burst in a negligibly short time, the escaping gas had an initially curved front. The possibility that the diaphragm when punctured at its center released the gas near the center before that near the edges cannot be overlooked.

(2) Non-simultaneous rupture of multiple layers of cellophane used as diaphragm for the higher pressures. For the two losest pressures used, only a single thickness of cellophane constituted the diaphragm, and for the two intermediate pressures two thicknesses sufficed, while for the two highest pressures 4 and 6 thicknesses were needed. It is possible that the knife merely punctured the first sheet of the multiple layers and the pressure exerted on the remaining sheets caused them to rupture in succession, sending a train of compression or shock waves into the expansion chamber.

The second of these possible sources of secondary disturbance has, it is felt, been eliminated as a major source of variability by a set of subsidiary measurements with diaphragm materials other than the usual cellophane, and with multiple sheets of cellophane used when one would withstand the pressure. No effect of the multiplicity of the diaphragm on the shock velocity or the amount of decrease was noted within the variations which occurred with a single diaphragm, as indeed is evidenced further by the main set of measurements where single sheets of cellophane at the lower pressures were not associated with variations less than were multiple layers at the higher pressures.

The most probable source of variation in shock strength and amount of decrease in shock strength is thus believed to be associated with the pre-rupture shape of the diaphragm and the manner in which the gas is permitted to escape from the compression chamber.

2. Persistent decrease in shock strength. Aside from the increases and decreases in shock strength as secondary disturbances associated with diaphragm rupture coalesce with the main shock, there appears to be a decrease in shock strength of about 0.5 percent per meter which persists with continued travel through the tube. The sources of this dissipation are possibly small disturbances continuously produced at the wall of the tube where the gas moving through the tube behind the shock meets irregularities. These disturbances would consist of small rarefactions which would be continually traveling in the air behind the main shock toward the main shock and decreasing its strength as they coalesce with it. Further experiments with shock tubes of different size and with varying roughness of the walls are needed to support this explanation.

The measurements described herein were performed at Princeton University in the summer of 1947 by F. B. Harrison and the author. The stimulation and support of the work by W. Bleakney, G. T. Reynolds, and A. Taub is appreciated.

APPENDIX

Distance and time measurements for shocks of various strengths appear in Table I. The four detection stations are numbered 1, 2, 3, and 4, in the order of increasing distance from the shock tube diaphragm. The symbols used in the table have the following meanings:

P_c - compression chamber gauge pressure before diaphragm rupture

S_2-S_1, etc. - distances between detection stations

t_2-t_1, etc. - time intervals between transits

$\Delta t = (t_4-t_3) - (t_2-t_1)$ = difference in time of travel over nearly equal distances at two places in shock tube

H - relative humidity

T - temperature of shock tube near first detection station

ΔT = temperature near first detection station minus temperature near third detection station

Δt^* - adjusted average value of Δt to represent difference in time of travel over equal distances of 0.7618 m at the two places in shock tube and to take into account temperature variation along tube as follows:

For a normal shock[L], $V^2 = a^2 \left(1 + \frac{\gamma+1}{2\gamma} z\right)$, where V is shock velocity, a is sound velocity, γ is ratio of heat capacities, $z = (p_2-p_1)/p_1$ is shock strength, i. e., fractional increase in pressure behind shock over that in front of shock. Using $\gamma = 1.4$ for air, $V^2 = a^2\left(1 + \frac{6}{7} z\right)$. z in these experiments ranges from 0.05 to 0.7, and V thus ranges between 1.00 a and 1.27 a. Variations in

---

L. Liepmann and Puckett, "Introduction to Aerodynamics of a Compressible Fluid", p. 40, Wiley, 1947.

temperature of the air in the tube lead to variations in accordance with $a = \sqrt{\gamma RT}$, where R is the gas constant and T Kolvin temperature. Thus, $\Delta a/a = \Delta T/2T$ which is at the most 0.05 percent. The effect on Δt of the small average measured differences in temperature at the two positions is subtracted from the average of the measured values of Δt for a given P_c and arrangement of detection stations.

$$k = \frac{\Delta t^*}{(S_3-S_1)(t_2-t_1)}$$: = fractional loss in velocity of shock per meter of travel

Table I

Distance, time, and gas initial condition data

shot serial no.	$t_2 - t_1$ μsec	$t_3 - t_1$ μsec	$t_4 - t_3$ μsec	Δt μsec	ΔT C°	T °C	H percent
$P_c = 1600$ mm Hg, $S_2 - S_1 = 0.7618$ meter, $S_3 - S_1 = 5.4884$ m, $S_4 - S_3 = 0.7623$ m							
45	1742	12,628	1759	17	0.15	25.0	60
46	1746	12,668	1766	20	.10	"	"
47	1745	12,653	1765	20	.00	"	"
49	1742	12,630	1761	19	−.10	"	"
66	1729.5	12,592.5	1753.5	24	.10	26.2	64
68	1735	12,587	1754	19	.05	"	"
76	1731	12,601	1756.5	25.5	.10	24.4	57
81	1742	12,618	1757	15	"	25.0	"
98	1738.5	12,617.5	1754	15.5	−.10	"	68
99	1733	12,583	1754	21	"	"	"
100	1736	12,596	1758	22	"	"	"
$S_2 - S_1 = 0.7618$ meter, $S_3 - S_1 = 1.8291$ m, $S_4 - S_3 = 0.7623$ m							
127	1752	4210.5	1757	5	.05	24.5	79
128	1753.5	4216	1759.5	6	"	24.55	"
133	1754	4217	1760.5	6.5	.00	24.6	"
134	1754	4216	1760	6	.05	24.65	"
139	1755	4216	1759	4	.10	24.8	80
140	1758.5	4225	1762.5	4	"	"	"
146	1752	4210	1756	4	−.05	25.3	79
154	1764	4238.5	1766.5	2.5	.10	23.0	76
$P_c = 1200$ mm Hg, $S_2 - S_1 = 0.7618$ m, $S_3 - S_1 = 5.4884$ m, $S_4 - S_3 = 0.7623$ m							
73	1807	13,084	1819	12	.15	24.15	56
77	1805.5	13,071	1820	14.5	.05	24.55	"
90	1805	13067	1818	13	.20	24.15	69

First group ($P_c = 1600$ mm Hg, $S_3 - S_1 = 5.4884$ m):

average $\Delta t = 19.8 \pm 5.7$ μsec

$\Delta t^* = 18.6 \pm 5.7$ μsec

(on basis of average $\Delta T = 0.08$ C°)

$k = (1.93 \pm .59) \times 10^{-3}$ per meter

Second group ($S_3 - S_1 = 1.8291$ m):

average $\Delta t = 4.8 \pm 2.3$ μsec

$\Delta t^* = 3.4 \pm 2.3$ μsec

(on basis of average $\Delta T = 0.05$ C°)

$k = (1.13 \pm .76) \times 10^{-3}$ per meter

Table I (continued)

shot serial no.	$t_2 - t_1$ μsec	$t_3 - t_1$ μsec	$t_4 - t_3$ μsec	Δt μsec	ΔT C°	T °C	H percent
$P_c = 1200$ mm Hg, $S_2 - S_1 = 0.7618$ m, $S_3' - S_1 = 5.4884$ m, $S_4 - S_3 = 0.7623$ m (continued)							
91	1805	13,078.5	1820.5	15.5	0.15	24.2	69
93	1804	13,063	1819	15	.20	24.4	"
97	1803	13,048	1815	12	−.05	25.0	"
107	1797	13,046	1815	18	−.10	25.2	"
110	1797	13,011	1811	13	.15	27.53	57

average $\Delta t = 14.1 \pm 3.9$ μsec
$\Delta t^* = 12.6 \pm 3.9$ μsec
(on basis of average $\Delta T = 0.09C°$)
$k = (1.26 \pm .39) \times 10^{-3}$ per meter

shot serial no.	$t_2 - t_1$ μsec	$t_3 - t_1$ μsec	$t_4 - t_3$ μsec	Δt μsec	ΔT C°	T °C	H percent
$S_2 - S_1 = 0.7618$ m, $S_3 - S_1 = 1.8291$ m, $S_4 - S_3 = 0.7623$ m							
147	1816	4369	1820	4	−.05	25.35	75
153	1823	4378	1825	2	.10	22.9	76
155	1822	4379	1826	4	.10	23.1	"
159	1821	4375	1825	4	.15	23.4	"
160	1820	4375	1825	4	.10	"	"
166	1819	4370	1822.5	3.5	.05	23.85	77

average $\Delta t = 3.6 \pm 1.6$ μsec
$\Delta t^* = 2.1 \pm 1.6$ μsec
(on basis of average $\Delta T = 0.07C°$)
$k = (0.63 \pm .48) \times 10^{-3}$ per meter

shot serial no.	$t_2 - t_1$ μsec	$t_3 - t_1$ μsec	$t_4 - t_3$ μsec	Δt μsec	ΔT C°	T °C	H percent
$P_c = 800$ mm Hg, $S_2 - S_1 = 0.7618$ m, $S_3 - S_1 = 5.4884$ m, $S_4 - S_3 = 0.7623$ m							
44	1890	13,667	1900	10	.15	24.7	59
53	1888.5	13,645	1898.5	10	.05	25.35	63
54	1889	13,644.5	1897.5	8.5	.10	25.4	"
55	1888.5	13,645.5	1898	9.5	.05	25.5	"
61	1885.5	13,630	1895	9.5	"	26.0	"
67	1885	13,631	1895	10	.10	26.2	"
78	1889.5	13,654	1900	10.5	.00	24.6	56
92	1890.5	13,659.5	1899	8.5	.20	24.3	68
105	1889	13,652	1897	8	−.10	25.3	"
108	1885	13,633	1894	9	.15	25.45	"
118	1880	13,525	1890	10	.10	27.05	56

average $\Delta t = 9.4 \pm 1.4$ μsec
$\Delta t^* = 7.9 \pm 1.4$ μsec
(on basis of average $\Delta T = 0.08C°$)
$k = (0.76 \pm .13) \times 10^{-3}$ per meter

Table I (continued)

P_c = 800 mm Hg (continued) $S_2 - S_1 = 0.7618$ m, $S_3 - S_1 = 1.8291$ m, $S_4 - S_3 = 0.7623$ m

shot serial no.	$t_2 - t_1$ μsec	$t_3 - t_1$ μsec	$t_4 - t_3$ μsec	Δt μsec	ΔT C°	T °C	H percent
145	1892	4549	1895.5	3.5	−0.10	25.2	73
152	1902	4570	1906	4	.05	27.85	76
156	1900.5	4566	1905	4.5	.15	23.2	〃
158	1900	4565	1903	3	.10	23.3	〃
165	1897	4559	1901	4	.05	23.8	〃

average $\Delta t = 3.8 \pm 0.8$ μsec
$\Delta t^* = 2.4 \pm 0.8$ μsec
(on basis of average $\Delta T = 0.05$ C°)
$k = (0.69 \pm .23) \times 10^{-3}$ per meter

P_c = 400 mm Hg, $S_2 - S_1 = 0.7618$ m, $S_3 - S_1 = 5.4884$ m, $S_4 - S_3 = 0.7623$ m

shot serial no.	$t_2 - t_1$ μsec	$t_3 - t_1$ μsec	$t_4 - t_3$ μsec	Δt μsec	ΔT C°	T °C	H percent
43	2002	14,518	2017	15	.20	24.7	58
52	2010.5	14,494.5	2016.5	6	.00	25.0	63
56	1998.5	14,491.5	2009	10.5	.10	25.6	〃
62	2008	14,486.5	2012	4	〃	26.1	〃
63	2006.5	14,477.5	2011	4.5	〃	〃	〃
64	2006	14,482	2007	1	〃	26.15	〃
75	2004.5	14,510	2016	11.5	.05	24.35	56
80	2008	14,490	2013	5	〃	24.85	〃
89	2011	14,514	2017	6	.20	24.05	68
102	2006	14,497	2010	4	−.15	25.05	〃
106	2006	14,491	2013	7	−.10	25.35	〃

average $\Delta t = 6.8 \pm 8.2$ μsec
$\Delta t^* = 5.3 \pm 8.2$ μsec
(on basis of average $\Delta T = 0.06$ C°)
$k = (0.48 \pm .74) \times 10^{-3}$ per meter

$S_2 - S_1 = 0.7618$ m, $S_3 - S_1 = 1.8291$ m, $S_4 - S_3 = 0.7623$ m

shot serial no.	$t_2 - t_1$ μsec	$t_3 - t_1$ μsec	$t_4 - t_3$ μsec	Δt μsec	ΔT C°	T °C	H percent
126	2012.5	4835	2016.5	4	.05	24.45	79
129	2012	4835	2016	4	〃	24.55	〃
132	2012	4834	2008.5	−3.5	.00	24.6	〃
135	2012.5	4835.5	2017	4.5	.05	24.7	〃
138	2011	4832	2015	4	〃	24.75	〃
141	2011.5	4832.5	2015	3.5	.10	24.8	〃
148	2006	4820	2010	4	−.05	25.35	75
167	2015	4842	2017	2	.05	23.9	77

ignoring measurement #132,
average $\Delta t = 3.7 \pm 1.7$ μsec
$\Delta t^* = 2.3 \pm 1.7$ μsec
(on basis of average $\Delta T = 0.04$ C°)
$k = (0.62 \pm .46) \times 10^{-3}$ per meter

Table I (continued)

shot no.	$t_2 - t_1$ μsec	$t_3 - t_1$ μsec	$t_4 - t_3$ μsec	Δt μsec	ΔT C°	T °C	H percent
$P_c = 200$ mm Hg, $s_2 - s_1 = 0.7618$ m, $s_3 - s_1 = 5.4884$ m, $s_4 - s_3 = 0.7623$ m							
50	2093	15,087	2096	3	0.00	24.85	63
51	2093	15,089	2096	3	"	24.9	"
57	2089	15,078	2092.5	3.5	.05	25.65	"
58	2086.5	15,069.5	2094.5	8	.10	25.75	"
65	2086	15,163.5	2090.5	4.5	.05	26.15	"
79	2091	15,084.5	2098.5	7.5	.00	24.7	56
87	2094.5	15,122.5	2097	2.5	.20	23.8	69
95	2091.5	15,103	2095.5	4	.15	24.5	"
101	2090	15,083	2093	3	−.15	25.05	"
$s_2 - s_1 = 0.7618$ m, $s_3 - s_1 = 1.8291$ m, $s_4 - s_3 = 0.7623$ m							
144	2090	5022.5	2092	2	.05	25.2	73
150	2101	5046	2102	1	.10	22.75	76
157	2098	5040	2100	2	.15	23.25	"
162	2095	5035	2098	3	.15	23.6	"
163	2095	5033	2098	3	.10	"	"
164	2096	5035	2099	3	.10	23.8	"
$P_c = 100$ mm Hg, $s_2 - s_1 = 0.7618$ m, $s_3 - s_1 = 5.4884$ m, $s_4 - s_3 = 0.7623$ m							
36	2160	15,556	2162	2	.35	21.05	69
38	2148	15,483	2150	2	.15	24.25	60
39	2148	15,481	2150	2	.20	24.4	"
40	2146	15,476	2149	3	"	24.5	"
41	2146	15,470	2146	0	.15	"	"
42	2148	15,480	2147	−1	"	24.55	"
60	2143.5	15,446.5	2141.5	−2	.10	25.85	63
69	2141.5	15,431	2140.5	−1	.00	26.2	"
88	2148.5	15,489.5	2149	0.5	.20	23.9	69
96	2144	15,460	2145	1	.10	24.5	"
103	2145	15,460	2145	0	−.10	25.1	"
109	2143	15,443	2144	1	.05	26.3	57

First group ($P_c = 200$ mm Hg, $s_3 - s_1 = 5.4884$ m):

average $\Delta t = 4.3 \pm 3.7$ μsec
$\Delta t^* = 2.8 \pm 3.7$ μsec
(on basis of average $\Delta T = 0.04$ C°)
$k = (0.24 \pm .32) \times 10^{-3}$ per meter

Second group ($s_3 - s_1 = 1.8291$ m):

average $\Delta t = 2.3 \pm 1.3$ μsec
$\Delta t^* = 0.6 \pm 1.3$ μsec
(on basis of average $\Delta T = 0.11$ C°)
$k = (0.16 \pm .34) \times 10^{-3}$ per meter

Third group ($P_c = 100$ mm Hg):

average $\Delta t = 0.6 \pm 2.6$ μsec
$\Delta t^* = -1.26 \pm 2.6$ μsec
(on basis of average $\Delta T = 0.13$ C°)
$k = -(0.77 \pm .22) \times 10^{-3}$ per meter

Table I (continued)

Serial no.	$t_2 - t_1$ μsec	$t_3 - t_1$ μsec	$t_4 - t_3$ μsec	Δt μsec	ΔT C°	T °C	H percent
P_c = 100 mm Hg (continued)			$s_2 - s_1 = 0.7618$ m,		$s_3 - s_1 = 1.8291$ m,		$s_4 - s_3 = 0.7623$ m
135	2144	5145	2145.5	1.5	0.05	24.45	79
130	2145.5	5148	2147	1.5	.10	24.6	"
131	2142.5	5144.5	2146	3.5	.05	"	"
136	2144	5144	2146	2	"	24.7	"
137	2144	5145.5	2146.5	2.5	.10	24.75	"
142	2145	5146	2146	1	"	24.8	"
143	2143	5137	2143	3	.00	25.15	73
149	2151	5164	2155	4	.10	22.65	76

average $\Delta t = 2.4 \pm 1.6$ μsec

$\Delta t^* = 0.7 \pm 1.6$ μsec

(on basis of average $\Delta T = 0.07$ C°)

$k = (0.18 \pm .41) \times 10^{-3}$ per meter

Table II

Average and derived quantities from shock velocity loss measurements.

P_c mm Hg	distance interval of measurement meters	V average shock velocity m/sec	H average relative humidity percent	T average temperature °C	a average sound velocity m/sec	z average shock strength	k (X100) percent velocity loss per meter of travel	$\frac{1}{z}\frac{dz}{dx}$ (X100) percent decrease in shock strength per meter of travel
1600	5.4884	435.04	62	25.2	347.4	.663	.193 ± .059	1.07 ± .32
	1.8291	433.58	79	24.5	347.2	.653	.113 ± .076	.63 ± .42
1200	5.4884	420.37	64	24.8	347.1	.545	.126 ± .039	.79 ± .24
	1.8291	418.22	76	23.7	346.6	.532	.063 ± .048	.40 ± .31
800	5.4884	402.50	63	25.4	347.5	.399	.076 ± .013	.60 ± .10
	1.8291	400.96	75	24.7	347.3	.389	.069 ± .023	.55 ± .18
400	5.4884	378.63	63	25.2	347.4	.219	.048 ± .074	.61 ± .94
	1.8291	378.44	78	24.6	347.3	.218	.062 ± .046	.78 ± .58
200	5.4884	363.55	64	25.0	347.3	.112	.024 ± .032	.55 ± .73
	1.8291	363.26	75	23.7	346.6	.115	.016 ± .034	.36 ± .76
100	5.4884	354.71	63	24.7	347.1	.049	−.011 ± .022	−.55 ± 1.09
	1.8291	355.39	78	24.5	347.2	.056	.018 ± .041	.79 ± 1.79

Reproduced by

DOCUMENT SERVICE CENTER

ARMED SERVICES TECHNICAL INFORMATION AGENCY

U. B. BUILDING, DAYTON, 2, OHIO

REEL-C 7366

A.T.I 208346

"NOTICE: When Government or other drawings, specifications or other data are used for any purpose other than in connection with a definitely related Government procurement operation, the U.S. Government thereby incurs no responsibility, nor any obligation whatsoever; and the fact that the Government may have formulated, furnished, or in any way supplied the said drawings, specifications or other data is not to be regarded by implication or otherwise as in any manner licensing the holder or any other person or corporation, or conveying any rights or permission to manufacture, use or sell any patented invention that may in any way be related thereto."

UNCLASSIFIED

9/2 STI-ATI-208 346 402537 p2014 UNCLASSIFIED

30/3

AD-A800 028

Dept of Physics, Princeton U, N.J.

VELOCITY LOSS MEASUREMENTS ON SHOCKS IN A SHOCK TUBE, by R. J. Emrich. Tech Rpt. 18 Nov 48, [17]p, illus (Contract N6-ori-105, Task III)

DIV: Fluid Mechanics (9)
SEC: Compressibility (2)
DIV: Research & Research Equipment (30)
SEC: Instrumentation (3)

SUBJECT HEADINGS
Shock tubes
Shock waves
Fluid mechanics
* Viscosity
Shock Tubes

(Copies obtainable from ASTIA-DSC)

Proj NR-061-020

CFSTI, auth: ONR memo, 8Apr68

UNCLASSIFIED

9/2 STI-ATI-208 346 UNCLASSIFIED

30/3

Dept of Physics, Princeton U, N.J.

VELOCITY LOSS MEASUREMENTS ON SHOCKS IN A SHOCK TUBE, by R.J. Emrich. Tech Rpt, 18 Nov 48, [17]p, illus (Contract N6-ori-105, Task II)

DIV: Fluid Mechanics (9)
SEC: Compressibility (2)
DIV: Research & Research Equipment (30)
SEC: Instrumentation (3)

SUBJECT HEADINGS
Shock tubes
Shock waves
Fluid mechanics

(Copies obtainable from ASTIA-DSC)
Proj NR-061-020

UNCLASSIFIED